

Local-Site Dependency of Magneto-Chiral Dichroism in Enantiopure One-Dimensional Copper(II)-Chromium(III) Coordination Polymers

著者	Kouji Taniguchi, Shuhei Kishiue, Hiyoshi Miyasaka, Shojiro Kimura
journal or publication title	Journal of the Physical Society of Japan
volume	88
page range	093708-1-093708-3
year	2019-08-28
URL	http://hdl.handle.net/10097/00128833

doi: 10.7566/JPSJ.88.093708

Local-Site Dependency of Magneto-Chiral Dichroism in Enantiopure One-Dimensional Copper(II)-Chromium(III) Coordination Polymers

Kouji Taniguchi^{1,2*}, Shuhei Kishiue², Shojiro Kimura¹, and Hitoshi Miyasaka^{*1,2}

¹ *Institute for Materials Research, Tohoku University, 2-1-1 Katahira, Aoba-ku, Sendai 980-8577, Japan*

² *Department of Chemistry, Graduate School of Science, Tohoku University, 6-3 Aramaki-Aza-Aoba, Aoba-ku, Sendai 980-8578, Japan*

(Received ** *, 2019)

Magneto-chiral dichroism (MChD) is a nonreciprocal directional dichroism emerged by applying a magnetic field to chiral materials, which provides a clear distinction between light propagating parallel and antiparallel to the magnetic-field direction. So far the correlation between the metal origin magnetization and MChD signal has been reported in homometallic complexes bearing chiral ligands, but that in hetero-metal systems with short-range correlations has never been investigated. Here, we demonstrate that MChD in *d-d* transitions of Cu^{II} bearing chiral ligands in an cyano-bridged copper(II)–chromium(III) chain is mainly proportional to the magnetization of local Cu^{II} center, which involves intra-atomic transition, rather than to the ferromagnetically correlated spin magnetization.

In the recent years, there has been a surge of interest in the interplay between chirality and magnetism, such as chirality-induced spin selectivity¹⁾, magnetic skyrmion with topological spin textures²⁾, and magneto-chiral dichroism (MChD).³⁾⁻¹³⁾ Among them, MChD is a nonreciprocal directional optical phenomenon, in which the absorption coefficient/luminescence intensity of a chiral material for an unpolarized light (or a linearly polarized light) is modified depending on the relative light propagating direction (\mathbf{k}) to an applied magnetic field (\mathbf{H}); parallel or antiparallel configuration. Furthermore, the sign of MChD is also changed by the chirality ($\gamma^{R/L}$) of materials as noted in the formula of $\gamma^{R/L} \mathbf{k} \cdot \mathbf{H}$ ($\gamma^R = -\gamma^L$).⁵⁾ Therefore, one noticeable feature of MChD is that the chirality of materials could be detected as opposite sign of signals by a ubiquitous unpolarized light under a magnetic field without using circularly polarized light. In addition, considering the nature of MChD

being a synergistic effect between chirality and magnetism, it could be possible to get knowledge of magnetic behavior in the target material by measuring MChD spectra. In fact, the MChD signal sometimes scales with the magnetization of the material as investigated in several homometallic compounds so far.¹¹⁾⁻¹³⁾ However, it is not clear how the MChD signal reflects the magnetic characteristics in the case of heterometallic compounds with short-range magnetic correlations made through components metal ions. We therefore focused on an enantiopure set of one-dimensional heterometallic Cu(II)–Cr(III) coordination polymers with a ferromagnetic superexchange interaction between Cu²⁺ ($S = 1/2$) and Cr³⁺ ($S = 3/2$) through the chain reported by Sereda *et al.*¹⁴⁾ and conducted their magnetic field dependence of MChD for $d-d$ transitions. The compounds are $\{[\text{Cu}((1\text{S/R},2\text{S/R})\text{-chxn})_2][\text{Cr}(\text{CN})_6]_2\}_n \cdot n[\text{Cu}((1\text{S/R},2\text{S/R})\text{-chxn})_2(\text{H}_2\text{O})_2] \cdot m(\text{H}_2\text{O})$ (**1-S/R**) ($1\text{S/R},2\text{S/R}\text{-chxn} = \textit{trans}$ -cyclohexane-(1S/R,2S/R)-diamine).¹⁴⁾ In this study, we have found that the MChD signal is mainly proportional to the local magnetization of the magnetic ion at which the intra-atomic optical transition occurs.

The crystal structure of **1-S/R** was confirmed to be the same as that in the previous report by measuring powder X-ray diffraction patterns (see Fig. S1 in the supplemental materials).¹⁵⁾ Enantiopure coordination polymers of both **1-S** and **1-R** crystallize in the non-centrosymmetric triclinic space group $P1$.¹⁴⁾ As displayed in Fig. 1, the asymmetric unit of **1-S/R** consists of the one-dimensional (1D) zigzag chain constructed by a $[\text{Cu}((1\text{S/R},2\text{S/R})\text{-chxn})_2]^{2+}$ cation linked by $[\text{Cr}(\text{CN})_6]^{3-}$, forming a $[-\text{Cu}^{\text{II}}-\text{NC}-\text{Cr}^{\text{III}}-\text{CN}-]$ repeating motif, and an isolated $[\text{Cu}((1\text{S/R},2\text{S/R})\text{-chxn})_2(\text{H}_2\text{O})_2]^{2+}$ cation (i.e., the asymmetric unit is composed in a 2:2:1 ratio of $[\text{Cu}((1\text{S/R},2\text{S/R})\text{-chxn})_2]^{2+}$, $[\text{Cr}(\text{CN})_6]^{3-}$ and $[\text{Cu}((1\text{S/R},2\text{S/R})\text{-chxn})_2(\text{H}_2\text{O})_2]^{2+}$, respectively). The axial positions of the chain Cu^{II} unit and the isolated Cu^{II} complex cation are occupied by two *cis*-positioned cyano groups of $[\text{Cr}(\text{CN})_6]^{3-}$ and two H₂O molecules, respectively (Fig. 1).

The paramagnetic characteristic of **1-S** was checked by measuring temperature dependence of the magnetic susceptibility (χ). The χT value of **1-S** at 300 K is 5.18 cm³ K mol⁻¹, which is close to the value estimated from isolated three Cu²⁺ ($S = 1/2$) and two Cr³⁺ ($S = 3/2$) in **1-S** by assuming $g = 2$; 4.875 cm³ K mol⁻¹ (see Fig. S2 in the supplemental materials).¹⁵⁾ As reported in the previous literature, the rapid increase of χT was observed below 50 K, indicating ferromagnetic correlation between Cu²⁺ ($S = 1/2$) and Cr³⁺ ($S = 3/2$) through the chain without the onset of spontaneous magnetization (see Fig. S2 in the supplemental materials).¹⁵⁾

Figure 2a displays the optical absorption spectrum of **1-S** in 0 T at room temperature.

In the ultraviolet-visible (UV-VIS) light region, the two peak structures are observed at ~575 nm and at ~380 nm in the optical absorption spectrum, respectively (Fig. 2a). In Fig. 2b, to assign these observed peaks, the optical absorption spectrum of **1-S** is compared with those of the precursor containing Cu^{2+} , $[\text{Cu}((1\text{S},2\text{S})\text{-chxn})_2(\text{H}_2\text{O})_2](\text{NO}_3)_2$ (**Cu-pre-S**), and $\text{K}_3[\text{Cr}(\text{CN})_6]$ containing Cr^{3+} . In the spectra of **Cu-pre-S** and $\text{K}_3[\text{Cr}(\text{CN})_6]$, the peaks of *d-d* transition for Cu^{2+} and Cr^{3+} are observed at ~570 nm and at ~380 nm, respectively, as reported in the literatures.^{16),17)} Comparing the peak positions in the spectra of **1-S**, **Cu-pre-S** and $\text{K}_3[\text{Cr}(\text{CN})_6]$, the optical excitations at ~575 nm and at ~380 nm could be assigned as the *d-d* transitions of Cu^{2+} and Cr^{3+} in **1-S**, respectively. For the *d-d* transitions of Cu^{2+} bearing chiral ligands, the natural circular dichroism (NCD) is observed, indicating that the chiral molecule ((1S/R,2S/R)-chxn), which directly coordinates to Cu^{2+} (Fig. 1), produces detectable chiral potential at the Cu^{2+} sites in **1-S/R** (see Fig. S3 in the supplemental materials).¹⁵⁾ In contrast, the NCD signal was not observed for the *d-d* transitions of Cr^{3+} probably because the chiral molecule, (1S/R,2S/R)-chxn, does not directly coordinate to Cr^{3+} (Fig. 1) and the chiral component of potential at the Cr^{3+} sites would be almost negligible due to the far distance between the chiral (1S/R,2S/R)-chxn and Cr^{3+} . Thus, hereafter, we focus on the MChD in the *d-d* transitions at the Cu^{2+} sites.

The optical absorption measurements were performed to detect MChD under **H** in a Faraday configuration, in which **H** was parallel or antiparallel to the propagating vector of the transmitted light (**k**) (see Fig. S4 in the supplemental materials).¹⁵⁾ By reversing the direction of **H**, while keeping **k** direction fixed, the relative direction of **k** to **H**, $\mathbf{k}\cdot\mathbf{H}$, is switched between parallel and antiparallel configurations. Figures 3(a) and 3(b) display the absorbance (*A*) of **1-S** in the magnetic field and the normalized difference spectra of the absorbance ($\Delta A/A$) for **1-S/R** at 4.3 K between the opposite directions of **H**, namely, $H = \pm 1$ T, respectively. *A* and ΔA are defined as the averaged absorbance under a magnetic field $\pm H$ (i.e., $A \equiv \{A(+H)+A(-H)\}/2$) and the change in the absorbance for the reversal of **H** (i.e., $\Delta A \equiv A(+H)-A(-H)$), respectively. Since, in the Faraday configuration, the circular dichroism/circular birefringence generates a fake ΔA signal through coupling with the anisotropy of crystal in the low symmetry systems, such as triclinic ones, the polycrystalline samples of **1-S/R** were dispersed in the KBr pellets to conduct measurement under pseudo-isotropic condition through random orientation of micro crystals. In the $\Delta A/A$ spectra of **1-S/R**, non-zero signals are clearly observed in the *d-d* transitions of Cu^{2+} , indicating the $\mathbf{k}\cdot\mathbf{H}$ dependence of absorbance. Furthermore, the sign reversal of $\Delta A/A$ is confirmed in the

enantiomer pairs of **1-S** and **1-R**. These results indicate that MChD, the sign of which is expressed by the formula of $\gamma^{R/L}\mathbf{k}\cdot\mathbf{H}$ ($\gamma^R = -\gamma^L$), is observed in the $d-d$ transitions of Cu^{2+} in **1-S/R**. The opposite sign two peaks in $\Delta A/A$ for **1-S/R** could be ascribed to the MChD in the different $d-d$ transitions from the split d orbitals by the triclinic crystal field potential at Cu^{2+} sites.

Figure 4(a) shows the magnetic field (H) dependence of the normalized MChD signal ($\Delta A/A$) at 4.3 K for the $d-d$ transitions of Cu^{2+} in **1-S**. The magnitude of the MChD signal develops with increasing H and the H -dependence of $\Delta A/A$ at 625 nm is displayed in Fig. 4(b). The MChD signal of **1-S** gradually increases and shows saturating behavior. At 10 T, the MChD signal reaches up to about 3.8×10^{-3} ($\sim 0.38\%$) of the corresponding absorbance. In Fig. 4(b), the H -dependence of magnetization (M) at 4.3 K for **1-S** is also plotted to investigate the correlation between the MChD signal and magnetic characteristics. Similar to MChD signal, the saturating behavior of M is observed and the M reaches $8.2 \mu_{\text{B}}$ per formula unit of **1-S** (f.u.) at 7 T, which is about 91 % of the value estimated from three Cu^{2+} ($S = 1/2$) and two Cr^{3+} ($S = 3/2$) in **1-S** by assuming $g = 2$; $9 \mu_{\text{B}}/\text{f.u.}$ However, as shown in Fig. 4(b), the H -dependence of MChD signal and M does not scale each other. Here, considering that the MChD is observed in the intra-atomic $d-d$ transition at Cu^{2+} sites in **1-S**, the MChD signal should be mainly dominated by the local electronic state of Cu^{2+} ($S = 1/2$). In fact, as shown in Fig. 4(b), we found that the H -dependence of MChD is well fitted with the Brillouin function for $S = 1/2$, which should be proportional to the magnetization estimated from isolated Cu^{2+} ions with $S = 1/2$ ($M_{\text{Cu(II)}}$). This result indicates that the contribution of magnetic interaction between Cu^{2+} ($S = 1/2$) and Cr^{3+} ($S = 3/2$) is negligible for the observation of MChD in the case of **1-S**.

In particular, if the magnetic interaction between Cu^{2+} ($S = 1/2$) and Cr^{3+} ($S = 3/2$) is negligible, the observed H -dependence of MChD signal is compatible with the microscopic model for MChD considering isolated Cu^{2+} ions. In the UV-VIS light region, the MChD is generally understood as an interference effect between electric dipole ($E1$) and magnetic dipole ($M1$) transitions.^{3),11)-13)} Based on this mechanism, the MChD signal of the $d-d$ transition for Cu^{2+} is expressed by the summation of the $E1$ - $M1$ interference term of optical transition from the two states with $S_z = \pm 1/2$ of the ground state for Cu^{2+} (see the supplemental materials for details).¹⁵⁾ Because the MChD signals from these two states with opposite sign of S_z cancel out each other (see the supplemental materials for details),¹⁵⁾ the ground states with $S_z = \pm 1/2$ of Cu^{2+} should be reflected in the MChD signal through the thermal

distribution of electrons, N_P and N_{AP} , in the two Zeeman splitting states. Here, N_P and N_{AP} represent the occupied number of the two states of Cu^{2+} with the H -parallel and the H -antiparallel magnetic moments, respectively. Taking account that the $M_{\text{Cu(II)}}$ is proportional to $N_P - N_{AP}$, the MChD signal of the $d-d$ transition for Cu^{2+} should scale with the $M_{\text{Cu(II)}}$.

In conclusion, the MChD for optical absorption in the visible light region was detected for the $d-d$ transition of Cu^{2+} in chiral paramagnetic one-dimensional heterometallic Cu(II)–Cr(III) coordination polymers of **1-S** and **1-R** with ferromagnetic correlation between Cu^{2+} ($S = 1/2$) and Cr^{3+} ($S = 3/2$). We have found that the magnetic correlation between Cu^{2+} ($S = 1/2$) and Cr^{3+} ($S = 3/2$) is negligible for the MChD in the $d-d$ transition of Cu^{2+} in **1-S**. We have demonstrated that the magnetic field dependence of MChD for the $d-d$ transition of Cu^{2+} in **1-S** approximately scales with the Brillouin function for $S = 1/2$, which is expected for the isolated Cu^{2+} ions. In the case that the magnetic correlation between Cu^{2+} ($S = 1/2$) and Cr^{3+} ($S = 3/2$) is sufficiently strong, the magnetic field dependence of MChD would be observed as deviated one from the simple Brillouin function. These observed characteristics may lead to the application of MChD as an element selective magnetic characteristic probe using a ubiquitous unpolarized light.

Acknowledgment

We acknowledge the supported by a Grant-in-Aid for Scientific Research on Innovative Areas (Grant no. JP17H05350; ‘Coordination Asymmetry’ Area 2802, Grant no. JP17H05137, ‘ π -System Figuration’ Area 2601), Grants-in-Aid for Scientific Research (Grant Nos. 16H02269, 16K05738 and 17H02917) from JSPS, a Support Program for Interdisciplinary Research (FRIS project), and the E-IMR project, the Murata science foundation. This work was partly performed at the High Field Laboratory for Superconducting Materials, Institute for Materials Research, Tohoku University (Project No 18H0404).

*E-mail: taniguchi@imr.tohoku.ac.jp, miyasaka@imr.tohoku.ac.jp

- 1) B. Göhler, V. Hamelbeck, T. Z. Markus, M. Kettner, G. F. Hanne, Z. Vager, R. Naaman and H. Zacharias, *Science*, **331**, 894 (2011).
- 2) S. Mühlbauer, B. Binz, F. Jonietz, C. Pfleiderer, A. Rosch, A. Neubauer, R. Georgii and P. Böni, *Science* **323**, 915 (2009).
- 3) L. D. Barron and J. Vrbancich, *Mol. Phys.*, **51**, 715 (1984).
- 4) G. L. J. A. Rikken and E. Raupach, *Nature*, **390**, 493 (1997).
- 5) G. L. J. A. Rikken and E. Raupach, *Phys. Rev. E*, **58**, 5081 (1998).
- 6) C. Train, R. Gheorghe, V. Krstic, L.-M. Chamoreau, N. S. Ovanesyan, G. L. J. A. Rikken, M. Gruselle and M. Verdaguer, *Nat. Mater.*, **7**, 729 (2008).
- 7) M. Saito, K. Ishikawa, K. Taniguchi and T. Arima, *Phys. Rev. Lett.*, **101**, 117402 (2008).
- 8) Y. Kitagawa, H. Segawa and K. Ishii, *Angew. Chem. Int. Ed.*, **50**, 9133 (2011).
- 9) M. Ceolín, S. Coberna-Ferrón and J. R. Galán-Mascarós, *Adv. Mater.*, **24**, 3120 (2012).
- 10) S. Kibayashi, Y. Takahashi, S. Seki and Y. Tokura, *Nat. Commun.*, **5**, 4583 (2014).
- 11) R. Sessoli, M.-E. Boulon, A. Caneschi, M. Mannini, L. Poggini, F. Wilhelm and A. Rogalev, *Nat. Phys.*, **11**, 69 (2015).
- 12) N. Nakagawa, N. Abe, S. Toyoda, S. Kimura, J. Zaccaro, I. Gautier-Luneau, D. Luneau, Y. Kousaka, A. Sera, M. Sera, K. Inoue, J. Akimitsu, Y. Tokunaga and T. Arima, *Phys. Rev. B*, **96**, 121102(R) (2017).
- 13) K. Taniguchi, M. Nishio, S. Kishiue, P.-J. Huang, S. Kimura and H. Miyasaka, *Phys. Rev. Materials*, **3**, 045202 (2019).
- 14) O. Sereda, J. Ribas and H. Stoeckli-Evans, *Inorg. Chem.*, **47**, 5107 (2008).
- 15) (Supplemental Material) The details of the experimental methods, characterization and discussion based on the microscopic model of MChD.
- 16) P. Sureshbabu, A. A. J. S. Tjakraatmadja, C. Hanmandlu, K. Elavarasan, N. Kulak and S. Sabiah, *RSC Adv.*, **5**, 22405 (2015).
- 17) J. J. Alexander and H. B. Gray, *J. Am. Chem. Soc.*, **90**, 4260 (1968).

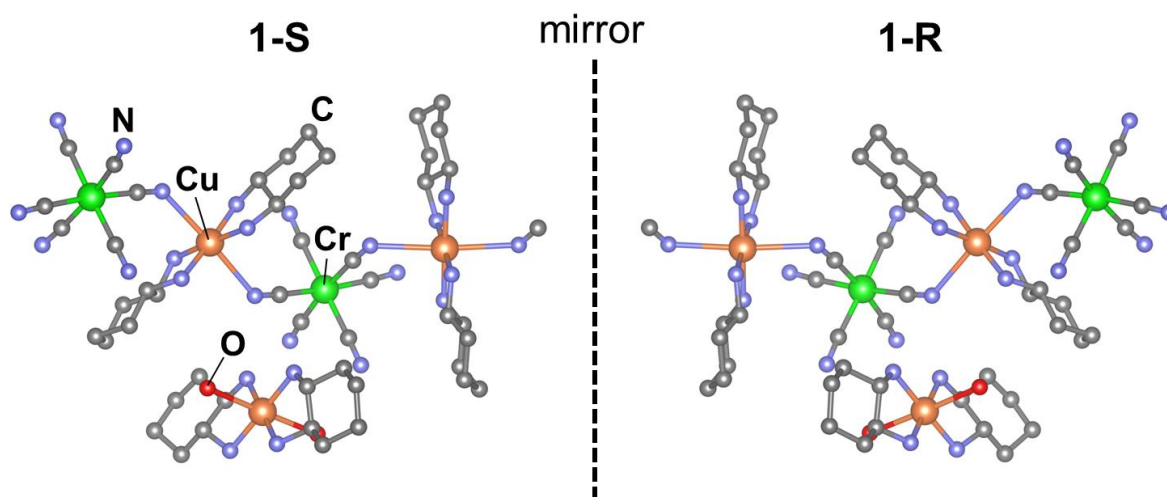


Fig 1. (Color online) Molecular structure of one dimensional heterometallic Cu(II)Cr(III) coordination polymers, **1-R/1-S**. Hydrogen atoms are omitted for clarity.

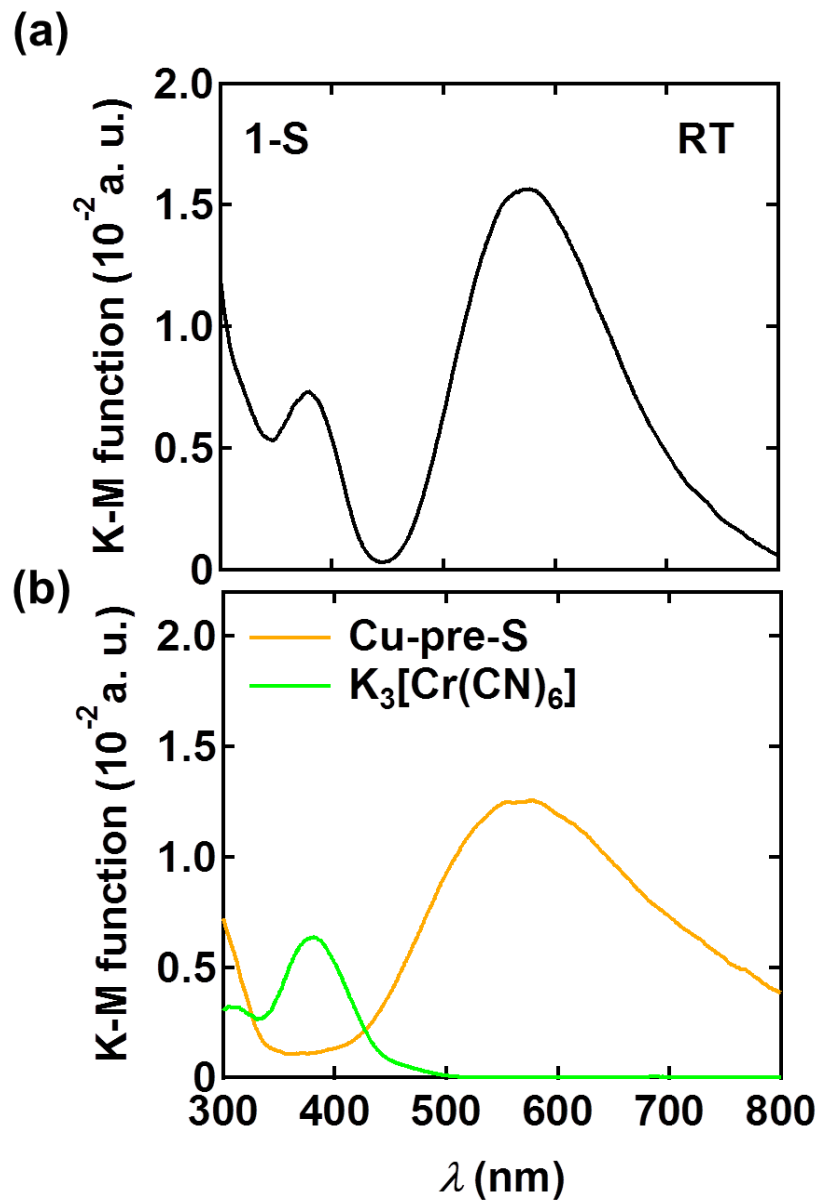


Fig 2. (Color online) (a) Optical absorption spectrum of **1-S** at room temperature in 0 T. (b) Optical absorption spectra of the precursor of **1-S** containing Cu^{2+} (**Cu-pre-S**) (orange line) and $\text{K}_3[\text{Cr}(\text{CN})_6]$ (yellowish green line) at room temperature in 0 T. Kubelka-Munk function (K-M function) was obtained by diffuse reflection measurements.

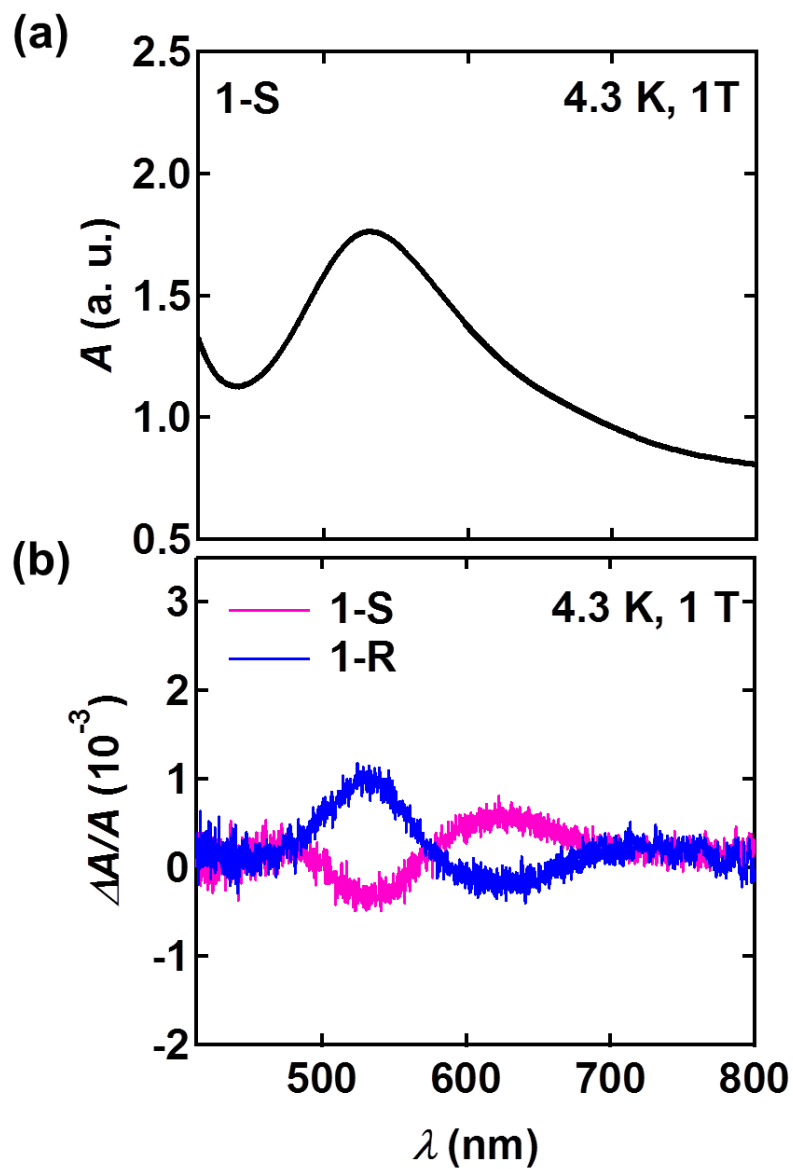


Fig 3. (Color online) (a) The averaged absorbance spectrum of **1-S** in KBr-pellet at 4.3 K in 1 T, where $A \equiv \{A(+1T) + A(-1T)\}/2$. (b) MChD spectra of **1-S** (blue line) and **1-R** (pink line) at 4.3 K in 1 T, where $\Delta A \equiv A(+1T) - A(-1T)$. The signal intensity is normalized by the averaged absorbance, A , in 1 T.

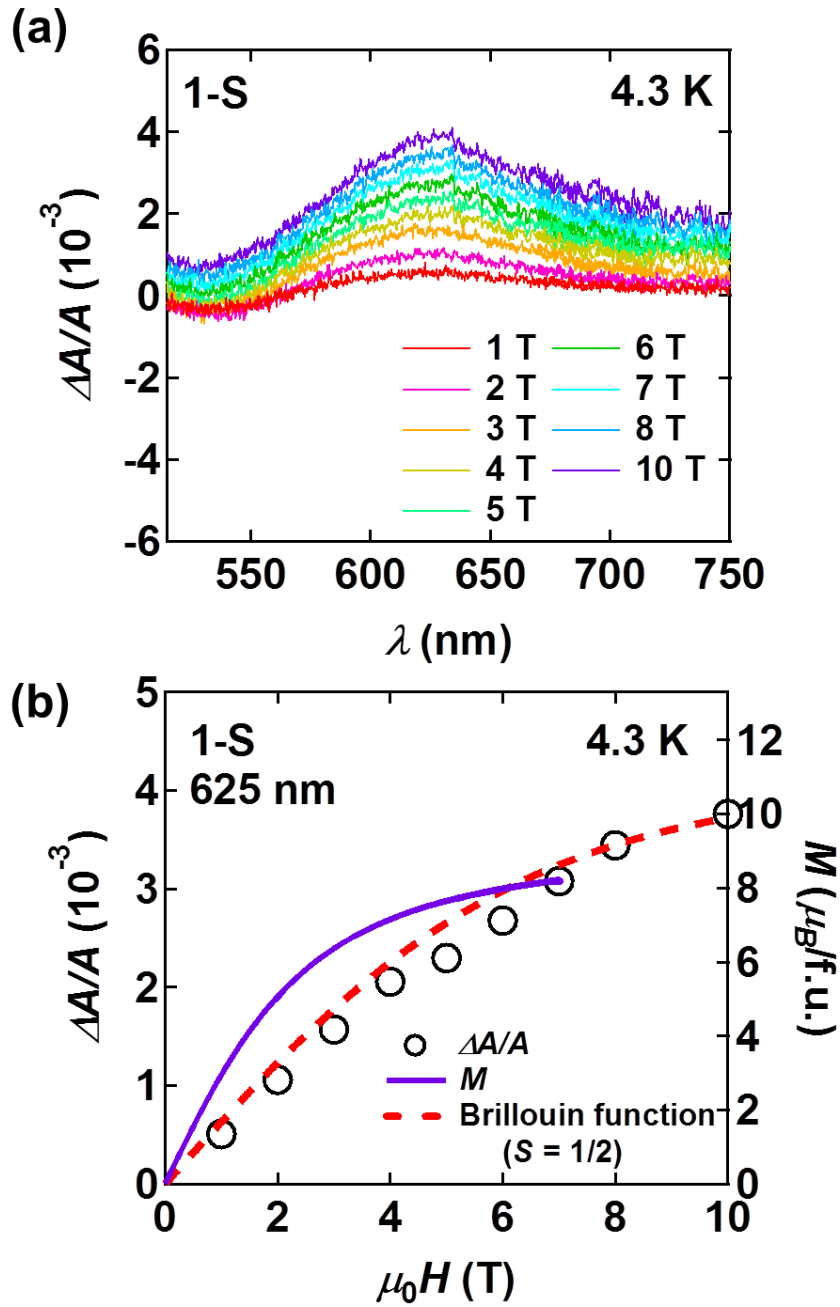


Fig 4. (Color online) Magnetic field dependence of the normalized MChD signal in absorbance. (a) MChD spectra of **1-S** at 4.3 K. The MChD signals for $d-d$ transition of Cu^{2+} are displayed. (b) Magnetic field dependence of $\Delta A/A$ at 625 nm (open circles) and magnetization (M) of **1-S** (purple line) at 4.3 K. The red dashed line displays the curve fitting result for the H -dependence of MChD signal by Brillouin function for $S = 1/2$.